EPJ Web of Conferences **66**, 03034 (2014)
DOI: 10.1051/epjconf/ 20146603034

Study of the structure of the Hoyle state by refractive α-scattering

S.A. Goncharov[1a], A.S. Demyanova[2], Yu.A. Gloukhov[2], A.N. Danilov[2], A.A. Ogloblin[2], T.L. Belyaeva[3], Yu.G. Sobolev[4], W. Trzaska[5], G.P. Tuyrin[5], and S.V. Khlebnikov[6]

[1]Lomonosov Moscow State University, Russia,
[2]NRC "Kurchatov Institute", Moscow, Russia,
[3]Universidad Autonoma del Estado de Mexico, Mexico
[4]JINR, Moscow region, Russia
[5]JYFL, Jyvaskyla, Finland
[6]Khlopin Radium Inst, St.-Peterburg, Russia

Abstract. α + ^{12}C elastic and inelastic to the Hoyle state (0^+_2, 7.65 MeV) differential cross-sections were measured at the energies 60 and 65 MeV with the aim of testing the microscopic wave function [1] widely used in modern structure calculations of ^{12}C. Deep rainbow (Airy) minima were observed in all four curves. The minima in the inelastic angular distributions are shifted to the larger angles relatively those in the elastic ones, which testify the radius enhancement of the Hoyle state. In general, the DWBA calculations failed to reproduce the details of the cross sections in the region of the rainbow minima in the inelastic scattering data. However, by using the phenomenological density with rms radius equal 2.9 fm, we can reproduce the Airy minimum positions.

1 Introduction and experimental data

The structure of the 0^+_2, 7.65 MeV "Hoyle" state of ^{12}C permanently attracts attention due to its importance for understanding many features of clustering phenomena in nuclei. The microscopic wave function calculated by Kamimura [1] represents the basis of different theoretical approaches to the problem. However, some predictions made by using this wave function, e.g., the radius of the Hoyle state, were not confirmed by empirical data [2]. Thus additional tests are highly desirable. It is well known that the nuclear rainbow scattering is one of the most powerful instruments for studying the nuclei interior, so we used it for testing [1] in the inelastic α+^{12}C scattering to the Hoyle state. The elastic and inelastic to the 0^+_2 state differential cross sections were measured at the energies 65 and 60 MeV in the angular ranges where rainbow effects reveal themselves. A pronounced minima at about 70^o (65 MeV) and 75^o (60 MeV) were observed in the inelastic scattering angular distributions (Fig. 1) and identified as the rainbow (Airy) ones due to repetition of similar minima in the far components of the cross sections and the expected shift of the experimental minima with the energy (as 1/E). The Airy-minima observed in the elastic scattering cross sections (Fig.2) are located at smaller angles (44^o and 50^o), providing thus an indication to the enhanced radius of the Hoyle state [3,4].

[a] Corresponding author: gsa@srd.sinp.msu.ru

The measured differential cross sections are presented in Figs. 1,2 together with DWBA and optical model calculations excluding the elastic and inelastic transfer of ^{8}Be. Experimental minima in the scattering data that recognized as the Airy-minima are seen only in the far side components of the cross sections calculated with zero absorption. The cross sections at the angles larger than ~ 90^{o} are strongly influenced by the ^{8}Be transfer mechanism [5].

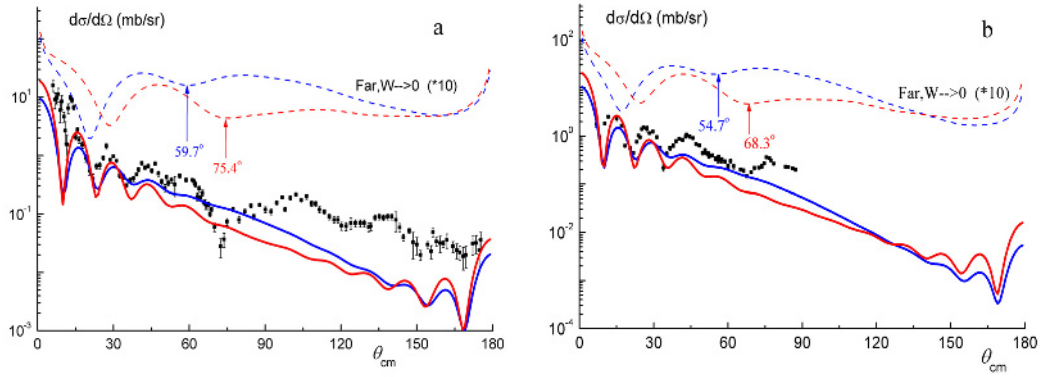

Figure 1. Differential cross sections of the inelastic α + ^{12}C scattering at (a) 60 and (b) 65 MeV leading to 0^{+}(7.65 MeV) state (in comparison with the DWBA calculations with the wave function from [1] (the blue solid line) and phenomenological transition density (the red solid line). Dashed lines correspond to the far components at W → 0.

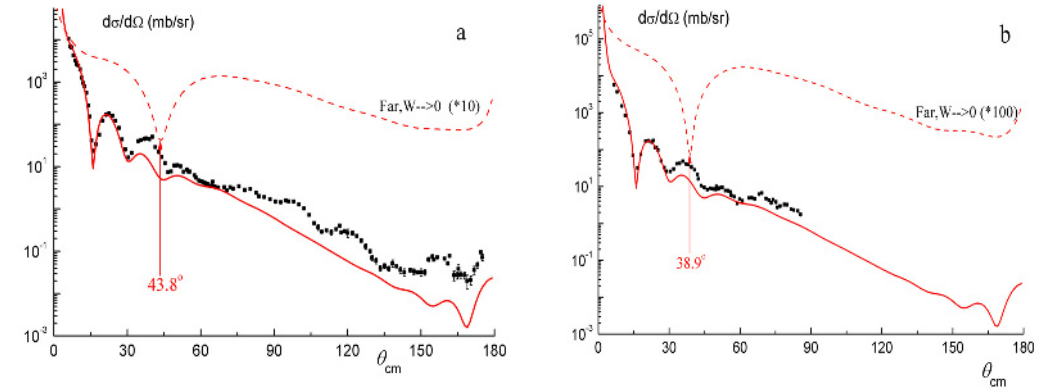

Figure 2. Differential cross section of α+^{12}C elastic scattering at (a) 60 and (b) 65 MeV. Calculations (the red solid line) are compared with our experimental data. Dashed lines correspond to the far components at W → 0.

2 Elastic scattering analysis

Unambiguously defined optical potentials describing the elastic scattering in the entrance and exit channels provide the most important basis for the analysis of the inelastic scattering. We used the semi-microscopic potentials obtained within the dispersive optical model (SMDOM) [6] for both channels. The SMDOM potential consists of three terms: 1) the real mean-field potential calculated in a microscopic folding model with corrected SNKE-approximation (for details see [5,6]); 2) the phenomenologically constructed complex Dynamic Polarization Potential (DPP) and 3) the Coulomb potential in the form of uniformly charged sphere. The folding potentials for the exit channel were calculated with the adopted material densities of the Hoyle state (see Section 3). The real ($V_{\rm i}$) and imaginary ($W_{\rm i}$) parts of the DPP use similar radial (Woods-Saxon) shapes for the volume terms and its derivatives for the surface ones. The energy dependent potential strengths ($V_{\rm S}(E)$, $W_{\rm S}(E)$), $V_{\rm D}(E)$ and $W_{\rm D}(E)$) were found by fitting all available elastic scattering data in a wide energy range. Due to

appearance of new data, we refined some parameters obtained before [5]. The parameters estimated by the energy dependence (Fig. 3) were used for the exit channel. Refined SMDOM-potentials, keeping the quality of the description of the angular distributions in the energy range from 40 to 240 MeV, better reproduce the data on the reaction cross sections, better suit the dispersion relations (Fig. 4) and well satisfy the inverse linear energy dependence of positions of the Airy-minimum (Fig. 5).

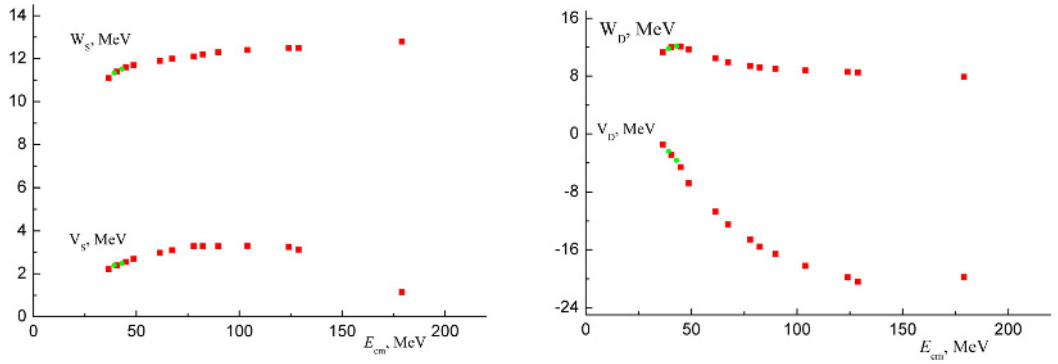

Figure 3. DPP parameters fitted to the elastic scattering data (the red squares) and estimated for the exit channels of inelastic scattering (the green circles).

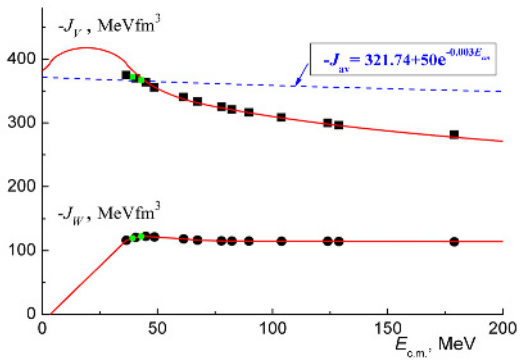

Figure 4. The fitted real and imaginary volume integrals of the SMDOM potentials. Green points are the estimated values. The red solid line in the upper part shows the sum of the dispersion integral and the volume integral of the mean field potential, the latter shown by the blue dashed line can be approximated analytically (see expression in the box).

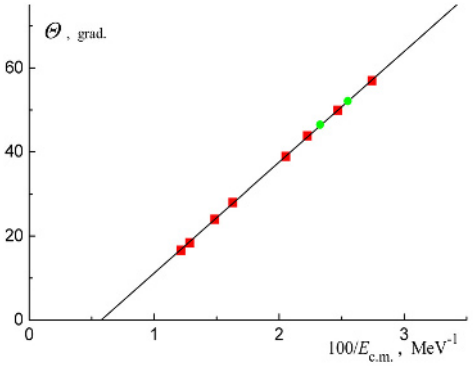

Figure 5. Positions of the Airy-minima for fitted (the red squares) and estimated DPP (the green circles), and linear approximation (the solid line)

3 Inelastic scattering analysis

The results of the DWBA analysis of the inelastic scattering data are shown in Fig.1. The inelastic form factor was taken in the form: $V_{if}(r) = V_{if}^{F}(r,E) + V_{if}^{C}(r)$. The first term represents the non-diagonal part of folding model potential, which was calculated as in [7]. The V_{if}^{C} describes the Coulomb excitation by standard way, and the reduced matrix element M(EL) is given by the known experimental value taken from [7].

Two approaches were used. As a first way, we calculated the material density of the excited state of 0^{+}_{2} (Fig. 6) and the transition density based on Kamimura wave functions [1] (Fig. 7). Fitting the data required renormalization of the transition density by $N = 0.4$ at both energies, 60 and 65 MeV.

As a second way we used the phenomenological models for the matter density of the state 0^+_2 and for the transition density. For the matter density (Fig. 6) we used a simple two-parameter Fermi form with the radius and diffusion parameters c = 2.88 fm and a = 0.5 fm leading to R_{rms} = 2.9 fm. This value is the same as the empirical one [2] and predicted by AMD [8], but significantly smaller than that given by [1] (3.53 fm). For the transition density we used the form of the parameterization based on the derivative of two-parametric Fermi form, which preserves the number of particles, but with the parameters c and a fitted to give the description of the angular distribution at angles up to 60° and the position of the first Airy-minimum in the far component. We have obtained the following values of parameters: c = 3.5 fm, a = 0.45 fm and parameter of renormalization ρ_0 = 0.005 at both energies 60 and 65 MeV (see Fig. 7).

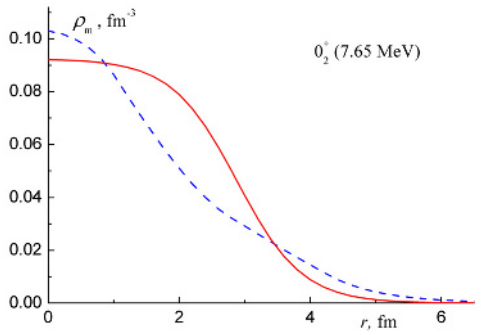

Figure 6. Microscopic [1] (the blue dashed line) and phenomenological (the red solid line) matter density distribution of the Hoyle state

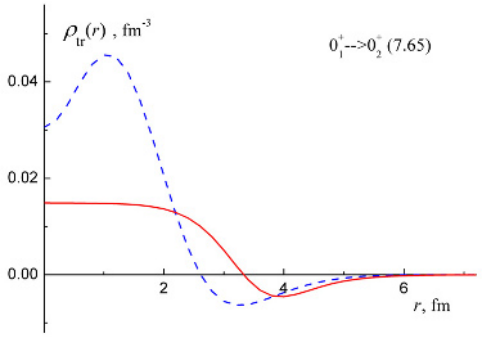

Figure 7. Renormolized microscopic [1] (the blue dashed line) and phenomenological (the red solid line) transition densities for excitation to the Hoyle state

Both calculations predict the appearance of the main Airy minimum at the angles larger than that in the corresponding elastic scattering angular distributions. However, Airy-minima are seen only in the far components of the calculated cross sections. The experimental cross sections are not reproduced in the rainbow minima regions. The reason of this is not completely clear. In particular, it can be attributed to a contribution of the ^{8}Be direct transfer mechanism, which is especially strong at the angles larger than 80° both in the elastic and inelastic scattering [5].

In general, our analysis led to two interesting results. First, it indicates to incomplete adequacy of the wave function [1], which produces too small rainbow angle in the inelastic scattering. Secondly, it shows that the rms radius of the state is not the only characteristic which defines the position of the Airy-minimum. The phenomenological transition density was used to predict the correct position of the minimum.

To conclude, the rainbow (Airy) minima were observed in the differential cross sections of the inelastic $\alpha+^{12}C(0^+_2$, 7.65 MeV) scattering. Their positions were reproduced by DWBA calculations with the phenomenological density distribution with the rms radius 2.9 fm that is the same as obtained in [2,8], and differs from the predictions given by microscopic Kamimura wave function [1].

The work was partly supported by grant 12-02-00927 of Russian Fund of Basic Researches.

References

1. M. Kamimura, Nucl. Phys. A **351**, 456 (1981)
2. A.N. Danilov *et al.*, Phys. Rev. C **80**, 054603 (2009)
3. S. Ohkubo and Y. Hirabayashi, Phys. Rev. C **70**, 041602(R) (2004)
4. A.S. Demyanova et al., IJMP E, **17**, 2118 (2008)
5. T.L. Belyaeva *et al.*, Phys. Rev. C **82**, 054618 (2010)
6. S. A. Goncharov and A. Izadpanah, Phys. At. Nucl **70**,18 (2007); **70**,1491 (2007)
7. D.T. Khoa and G.R. Satchler, Nucl. Phys. A **668**, 320 (2000)
8. T. Suhara and Y. Kanada-En'yo, PTP **123**, 303 (2010)